

## Research Article

# A Comprehensive Investigation on the Influence of Zeolite, Pumice, and Limestone Powder on the Characteristics of Eco-Friendly Calcium Aluminate Cement Mixes

A. R. Rasekhi Sahneh,<sup>1</sup> M. A. Dashti Rahmatabadi ,<sup>1</sup> H. Madani ,<sup>2</sup>  
and H. Dehghan Manshadi<sup>1</sup>

<sup>1</sup>Department of Civil Engineering, Yazd Branch, Islamic Azad University, Yazd, Iran

<sup>2</sup>Faculty of Civil and Surveying Engineering, Graduate University of Advanced Technology, Kerman, Iran

Correspondence should be addressed to H. Madani; [h.madani@kgut.ac.ir](mailto:h.madani@kgut.ac.ir)

Received 13 November 2022; Revised 30 December 2022; Accepted 17 March 2023; Published 19 April 2023

Academic Editor: Tanakorn Phoo-ngernkham

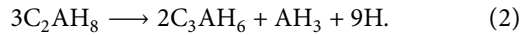
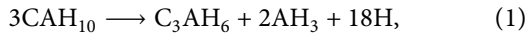
Copyright © 2023 A. R. Rasekhi Sahneh et al. This is an open access article distributed under the Creative Commons Attribution License, which permits unrestricted use, distribution, and reproduction in any medium, provided the original work is properly cited.

The current research aims to investigate the influence of pumice, zeolite, and limestone powder as supplementary cementitious materials (SCMs) on the characteristics of calcium aluminate cement (CAC) composites. For this purpose, SCMs were used in substitution levels of 5%, 15%, 25%, 40%, and 60% of CAC. The results indicate that the active SCMs had a great influence on enhancing the characteristics of the cement composites. For instance, the mixtures with 40% pumice and zeolite outperformed the plain mixture in the compressive strength test by about 45% and 90% at 90 days, respectively. At the age of 90 days, the rapid chloride migration coefficient for the optimal mixture of Z40 (containing 40% zeolite) was reduced by about 93%, and the electrical resistance was increased by about 70% in comparison to the age of 28 days; however, at the same ages, for the plain mixture, the rapid chloride migration coefficient was increased by about 74%, and the electrical resistance was decreased by about 60%. At the age of 90 days, the electrical resistivity of the Z40 mixture was 685% higher compared to the plain mixture. The results show that the high cost of CAC composite could be significantly lowered by utilizing SCMs. Moreover, using SCMs could significantly lower greenhouse gas emissions. In addition, the tests including the modulus of rupture, modulus of elasticity, permeable pore space, XRD, and microstructural analyses were also carried out to study the mechanical and durability properties. It must be mentioned that the effect of high dosages of pumice and zeolite on the durability properties of this type of cement has not been studied previously, which can be considered an innovation of this study. Furthermore, the obtained results could be beneficial to develop applications of CAC.

## 1. Introduction

Calcium aluminate cement (CAC) is an appropriate binder in the construction industry owing to its high abrasion resistance, high acid resistance, and high strength [1–6]. CAC concrete can be poured in a place like Portland cement and converted from liquid to solid at room temperature [7–9]. Furthermore, unlike the production of Portland cement, CAC production leads to lower emissions, which can be so beneficial regarding the environmental aspect [10]. CAC concretes are utilized in broad applications such as the refractory and building industry [10].

There are two main reasons for restricting the use of CAC cement. First, the hydration process in CAC cement is entirely different from that of the Portland cement. During the hydration process of CAC cement, stable phases such as  $AH_3$  (gibbsite) and  $C_3AH_6$ , metastable phases such as  $CAH_{10}$  and  $C_2AH_8$ , or a combination of these two phases can be produced [11–13]. As expressed in equations (1) and (2), the metastable phases are gradually converted into stable phases over time, known as conversion processes [11, 13, 14]. As a result, the porosity is increased, and the compressive strength is reduced [15].



Second, the cost of CAC production is higher than Portland cement due to the bauxite supply limitation. To make CAC cement a reliable alternative to Portland cement, these two challenges should be addressed.

Several studies have proposed different methods to suppress the conversion process, one of which is curing CAC concrete at high temperatures. The researches show that the stable phases ( $\text{C}_3\text{AH}_6$  and  $\text{AH}_3$ ) are formed at temperatures of 40–60°C, while the  $\text{CAH}_{10}$  phase is formed at temperatures below 20°C. Other studies also reported that  $\text{C}_2\text{AH}_8$  and  $\text{AH}_3$  phases are formed at temperatures of 20–40°C [16–20].

In recent years, supplementary cementitious materials (SCMs) have been widely used in the construction industry due to the capability of these materials to produce durable concrete with lower  $\text{CO}_2$  emissions [21]. A significant benefit of using SCMs is attributed to the environmental aspect of concrete production. Each year, large amounts of waste materials such as industrial wastes and dust are disposed to the environment, which this could be hindered by using these materials as SCMs in concrete [22–24]. The hydration mechanism of CAC-SCMs composite maybe changed by incorporation of SCMs. For instance, using SCMs such as ground granulated blast furnace slags may form the strätlingite ( $\text{C}_2\text{ASH}_8$ ) phase believing to mitigate the conversion process due to the high stability of this phase [25]. Kirca et al. [26] reported that the high-level incorporation of ground granulated blast furnace slags (more than 40%) in CAC composite could limit the conversion process without generating strength loss. In another study, Collepardi et al. [27] stated that incorporating 15% silica fume could reduce the strength loss because of the formation of strätlingite, which could mitigate the conversion of metastable phases.

As stated previously, the conversion process as an essential factor affecting the performance of the CAC cement needs to be studied; therefore, the main purpose of the present research is to study the effect of adding pumice, zeolite, and limestone powder as SCMs on the conversion process. As the conversion process cannot be directly tested, the effect of conversion process on the mechanical and durability properties has been evaluated. More specifically, pumice, zeolite, and limestone powder are used as supplementary cementitious materials in substitution levels of 5%, 15%, 25%, 40%, and 60%. During the current research, the compressive strength, modulus of rupture, modulus of elasticity, rapid chloride migration, electrical resistivity, permeable pore space, XRD, and microstructural analyses were performed to study the mechanical and durability properties. Additionally, a simple cost and environmental analyses were also carried out.

A lot of studies have investigated binary and ternary Portland cements; however, binary and ternary calcium aluminate cement composites have rarely been studied.

In particular, the effect of pumice, zeolite, and limestone powder on the durability of this type of cement has not been studied, which can be considered as an innovation of this study. The results can also be applicable in developing standards for calcium aluminate cement.

## 2. Experimental Program

**2.1. Materials Properties.** Calcium aluminate cement (manufactured by Kerneos Inc, France) was used in the mixtures. The chemical composition of the CAC is shown in Table 1. In this paper, natural sand was used as aggregate. In Tables 2 and 3, the properties of the natural sand are included. A polycarboxylate ether-based superplasticizer with a specific gravity of 1.1 g/cm<sup>3</sup> was used in this paper. The pumice, zeolite, and limestone powder were utilized as the SCMs. The chemical and physical properties of SCMs are provided in Table 1.

**2.2. Mix Design and Specimen's Preparation.** The mixtures were prepared at water to cementitious ratio of 0.4. The cement content was kept constant at a level of 550 kg/m<sup>3</sup>. High cost is a challenge of using calcium aluminate cement that needs to be addressed. In this regard, researchers have studied the effect of replacement at different levels (low to high). Available research shows that other studies have investigated the replacement level in the range of 15%–40% [26, 27]. In this study, SCMs were considered as a portion of cement in levels of 5%, 15%, 25%, 40%, and 60% by weight of cement. In the following notes, the method of preparing mixtures is provided:

- (i) Dry ingredients were mixed for 1.5 min.
- (ii) Adding water to the dry ingredients.
- (iii) Mixing the cement composite for 2 min and adding the required superplasticizer.
- (iv) Continuing mixing for another 4 min.
- (v) Mix proportions are shown in Table 4. It is worth mentioning that after casting, for minimizing water evaporation, all specimens were protected with a plastic sheet for 24 hours. After that, the samples were demolded and cured in water at a temperature of  $22 \pm 2^\circ\text{C}$ .

### 2.3. Test Methods

**2.3.1. Flowability.** The flowability test results were determined in accordance with ASTM C1437 [28]. In this paper, the desired flowability was considered in the range of  $19 \pm 1$  cm.

**2.3.2. Compressive Strength.** Compressive strength test results were carried out, according to BS EN12390-3 [29]. At each age, four cubic specimens with the dimension of 50 mm were tested.

TABLE 1: Physical properties and chemical composition of the cement, pumice, zeolite, and limestone.

Properties	SiO <sub>2</sub>	Fe <sub>2</sub> O <sub>3</sub>	Al <sub>2</sub> O <sub>3</sub>	CaO	MgO	SO <sub>3</sub>	Na <sub>2</sub> O	K <sub>2</sub> O	Specific gravity (g·cm <sup>-3</sup> )	BET surface area (cm <sup>2</sup> ·g <sup>-1</sup> )	LOI
CAC	4.25	10.14	43.45	40.3	0.61	0.05	0.09	0.1	3.24	3600	0.55
P	61	5	19	8	2.1	0.4	1.6	2	2.63	4500	0.9
Z	67.1	1.46	13.9	7.04	3.15	0.05	1.62	1.19	2.25	6800	2.1
L	1.47	0.29	0.22	54.77	1.2	0.06	0.05	0.08	2.69	3300	41.8

where P: pumice, Z: zeolite, L: limestone, CAC: calcium aluminate cement.

TABLE 2: Properties of the natural sand.

Properties	Maximum nominal size (mm)	SSD density (kg·m <sup>-3</sup> )	SSD water absorption (%)
Natural sand	4.75	2640	2.03

where SSD: saturated surface dry.

TABLE 3: Size gradation of the sand used in this study.

Sieve number	4	8	16	30	50	100	200
Cumulative percent passing	71.5	44.4	29.8	14.2	6.1	1.5	1.28

TABLE 4: The mortar mixture proportions.

Mix	CAC (kg·m <sup>-3</sup> )	Sand (SSD) (kg·m <sup>-3</sup> )	SCMs (kg·m <sup>-3</sup> )	Water (kg·m <sup>-3</sup> )	Superplasticizer (kg·m <sup>-3</sup> )	Flowability (cm)
Plain	550	1523	—	220	0	19.5
P5	522.5	1495.8	27.5	220	0.97	19.2
P15	467.5	1485.7	82.5	220	1.76	20
P25	412.5	1475.8	137.5	220	2.7	19.7
P40	330	1460.9	220	220	3.6	20
P60	220	1441.1	330	220	5	19.5
Z5	522.5	1491.2	27.5	220	1.2	18.5
Z15	467.5	1472.4	82.5	220	2.1	18.3
Z25	412.5	1453.5	137.5	220	4.68	18.7
Z40	330	1425.3	220	220	8.53	18.3
Z60	220	1387.6	330	220	17.95	19.1
L5	522.5	1496.2	27.5	220	0	18.2
L15	467.5	1487.5	82.5	220	0.1	19.1
L25	412.5	1478.7	137.5	220	0.24	19.4
L40	330	1465.6	220	220	0.39	18.9
L60	220	1448.1	330	220	1.08	19

2.3.3. *Rapid Chloride Migration Test (RCMT)*. RCMT was conducted in accordance with the NT BUILD492 [30]. After performing the test procedure according to the standard mentioned above, chloride ions penetration depth into the

specimen covered with 0.1M silver nitrate solution was measured by caliper. Then, the RCMT coefficient can be obtained using the following equation (3):

$$D_{\text{ncsm}} = \frac{0.0239(273 + T) \times L}{(U - 2) \times t} \times \left( X_d - 0.0238 \times \sqrt{\frac{(273 + T) \times L \times X_d}{U - 2}} \right), \quad (3)$$

where  $D_{\text{ncsm}}$ : RCMT coefficient,  $\times 10^{-12}$  m<sup>2</sup>/s,  $U$ : voltage, V,  $T$ : average temperatures in the anolyte solution at the initial and final stage, °C,  $L$ : thickness of specimen, mm,  $X_d$ : penetration depths, mm, and  $t$ : test duration, hour

2.3.4. *Electrical Resistivity*. The Wenner method (four-point method), which is the most common method for measuring the electrical resistivity of cement composites [31, 32], was employed to obtain the electrical resistivity of

specimens. 100 × 200 mm cylindrical specimens were used for this test. The Wenner apparatus has four surface electrodes located at equal distances from each other. To calculate the electrical resistance, the Wenner device is attached to the concrete sample's surface, and an electric current is conducted between the electrodes. Then, the electrical resistivity was obtained using the following equation [32]:

$$\rho = 2 \cdot \pi \cdot a \cdot \frac{\Delta V}{I}, \quad (4)$$

where  $I$ : electric current (A),  $a$ : distance between electrodes (cm),  $\Delta V$ : potential difference (V), and  $\rho$ : electrical resistivity (kΩ·cm)

**2.3.5. Modulus of Rupture.** The modulus of rupture test was measured in accordance with the BS-EN 196-1 [33]. In each age, three 40mm × 40mm × 160mm prismatic specimens were used. As required by the standard, the three-point loading method with a loading rate of 50 ± 10 N/s was used. The modulus of rupture was calculated according to the following equation [33]:

$$R_f = \frac{1.5 \times F_f \times L}{b^3}, \quad (5)$$

where  $R_f$ : modulus of rupture, MPa,  $b$ : the width of the specimen, mm,  $F_f$ : load at the middle point, N, and  $L$ : supports distance, mm.

**2.3.6. Modulus of Elasticity.** ASTM C469 [34] was used to measure the modulus of elasticity. To remove any surface irregularity and make sure that both ends of the specimens are perpendicular to the sides of the specimen, both ends were ground. The loading rate of 0.28 MPa/s was applied during the test. Strain-measuring equipment attached to two fixed rings was used for measuring deformation. The static elastic modulus of concrete was measured in accordance with the following equation:

$$E = \frac{\sigma_2 - \sigma_1}{\varepsilon_2 - 0.000050}, \quad (6)$$

where  $E$ : chord modulus of elasticity,  $\sigma_2$ : stress at 40% of the ultimate load,  $\sigma_1$ : stress at a longitudinal strain of 50 millionths, and  $\varepsilon_2$ : longitudinal strain caused by  $\sigma_2$ .

**2.3.7. Permeable Voids.** At 28 days of age, the ASTM C642 [35] method was used to determine the permeable voids content. The following process is specified according to the standard for determining the permeable voids. Cylindrical specimens with a diameter of 100 mm and a height of 50 mm were dried at 105°C until they reach a constant weight. Afterwards, the dried specimens were immersed in water until they reach a constant weight. Using the following equation, the permeable voids content can be determined.

$$\begin{aligned} \text{Permeable (\%)} &= \frac{g_2 - g_1}{g_2} \times 100, \\ g_1 &= \left| \frac{A}{(C - D)} \right| \times \rho, \\ g_2 &= \left| \frac{A}{(A - D)} \right| \times \rho, \end{aligned} \quad (7)$$

where  $A$ : the mass of dried sample (g),  $C$ : the mass of the surface-dry sample after immersion and boiling (g),  $D$ : apparent mass of sample in water after immersion and boiling (g),  $\rho$ : density of water (g/cm<sup>3</sup>),  $g_1$ : the dry bulk density (g/cm<sup>3</sup>), and  $g_2$ : the apparent density (g/cm<sup>3</sup>).

**2.3.8. Scanning Electron Microscopy (SEM).** SEM was employed to study the effect of SCMs as supplementary cementitious materials on the microstructure of mixtures in more details. TESCAN VEGA3 SEM apparatus was utilized to capture SEM images.

**2.3.9. Economic and Environmental Assessment.** Each mixture's cost and carbon footprint are estimated by adding up the prices and carbon footprints of its constituent parts. Equation (8) was used to compute the unit cost of each mixture.

$$M = \sum_i^n m_i g_i, \quad (8)$$

where  $M$ : unit cost of a mixture per cubic meter,  $m_i$ : unit cost of the  $i$ -th ingredient ( $i = 1, 2, 3, \dots, n$ ), and  $g_i$ : mass of the  $i$ -th ingredient of the mixture.

Equation (9) was used to determine the carbon footprint of each mixture:

$$\text{Global warming index} = \sum_i^n m_i \times GWP_i, \quad (9)$$

where global warming index is the carbon footprint of a mixture per cubic meter;  $GWP_i$ : unit carbon footprint of the  $i$ -th ingredient ( $i = 1, 2, 3, \dots, n$ ), and  $m_i$ : mass of the  $i$ -th ingredient of the mixture.

The unit cost and carbon footprint of the materials used in the investigated mixes are shown in Table 5. References [36–41] were used to compile the inventory data.

### 3. Results and Discussion

**3.1. XRD Analysis.** An X-ray diffraction experiment can reveal cement paste's crystalline structure [42]. Diffraction patterns for the investigated mixtures at 7 and 90 days of hydration are shown in Figure 1. As it is clear, the metastable phases  $CAH_{10}$  and  $C_2AH_8$  are identified at the age of 7 days in the plain mixture. The presence of these phases is highly correlated with high strength at an early age [42]. However, at the later age of 90 days, the metastable phases are not detected in the plain mixture, indicating that the metastable phases have been converted to the stable ones. This may lead

TABLE 5: Database used for unit cost and carbon footprint of raw materials.

Ingredients	Cost (USD/kg)	Carbon footprint (kg-CO <sub>2</sub> /kg)
CAC	1.8	0.72
Sand	0.01	0.002
Pumice	0.05	0.004
Zeolite	0.053	0.03
Limestone powder	0.039	0.027
SP	6	0.772
Water	0.005	0.001

to the decrease in strength of the plain mixture at the age 90 days.

At the age of 7 days, the XRD patterns for the mixtures containing zeolite, pumice, and limestone powder show the presence of the metastable and stable phases. In addition, the presence of the strätlingite ( $C_2ASH_8 \rightarrow 2CaO \cdot Al_2O_3 \cdot SiO_2 \cdot 8H_2O$ ) phase is detectable in mixtures containing 40% pumice and zeolite at the age of 7 days, demonstrating the reactivity of pumice and zeolite at an early age. Furthermore, at this age, it is clear that the metastable phases are lower in mixtures containing pumice and zeolite than in the plain mixtures, indicating that these materials effectively decrease the production of the metastable phases. The amount of the stable phase of strätlingite is increased with the age of mixtures, which could explain why these materials have an appropriate performance in the CAC composites. The findings indicate that adding limestone powder has little effect on the conversion process and does not prevent the formation of the metastable phases, which is in line with the compressive strength and durability results.

**3.2. The Compressive Strength.** The results from 1 day up to 90 days are represented in Figures 2 to 4. It is clear from the figures that the CAC composites have high compressive strength at early ages. The plain mixture has a compressive strength of more than 33 MPa at the age of 1 day. By increasing the age up to 28 days, the plain mixture has shown an increasing trend, reaching 44.5 MPa. Nevertheless, unlike the Portland cement mixture, by increasing the age up to 90 days, the CAC cement composite has shown a decreasing trend owing to the conversion processes. For instance, the compressive strength of the plain mixture was decreased by 45%.

The obtained results show that incorporating pumice, zeolite, and limestone powder, especially at high replacement levels, results in lower strengths at an early age. Moreover, replacing pumice and zeolite up to 15% has not prevented the reduction in compressive strength at later age; therefore, this percentage of replacement is not optimal and is not recommended. Similarly, the mixtures with limestone powder have a decreasing trend in compressive strength, which could be due to the lower activity of limestone powder in comparison to the pumice and zeolite powder.

The stable phases  $C_3AH_6$  and  $AH_3$  are the major reason for the long-term strength of calcium aluminate cement mixtures. During the hydration process at ambient

temperature, the metastable phases of  $CAH_{10}$  and  $C_2AH_8$  are formed earlier than stable phases. These metastable phases have a large amount of water in their structure and also have a low density enabling these phases to fill the space originally occupied by water and give high early strengths [14]. However, it should be mentioned that these early strengths, which may persist for several years, are transient due to the occurrence of the conversion process, which is thermodynamically inevitable. The conversion process is responsible for the long-term strength reduction of CAC cement composite [15].

The current results indicate that the mixtures containing zeolite have superior performance among all mixtures at the age of 90 days. In contrast, the mixtures containing limestone powder have the lowest compressive strength. At the age of 90 days, the results reveal that increasing the replacement level of pumice and zeolite up to 40% could enhance the compressive strength, but beyond 40%, the compressive strength has shown a decreasing trend. In this study, the optimal replacement level is found to be 40%; however, the negative effects of the conversion process are mitigated in proportions above 25% for mixtures containing pumice and zeolite. Furthermore, at the age of 90 days by increasing the replacement level of pumice and zeolite up to 60%, the compressive strength has decreased, but it is noteworthy that these mixtures still have a higher compressive strength than the plain mixture which can be considered as a positive characteristic in sustainable development. Additionally, zeolite is more effective than pumice in obtaining higher compressive strength. For example, the Z40 mixture has 30% better performance in comparison to the P40 mixture. The higher specific surface area of zeolite compared to pumice could be the reason for the higher reactivity of zeolite compared to pumice [43, 44].

As stated previously, by increasing the age of the mixtures to 90 days, the compressive strength of the plain mixture is 45% lower than that at the age of 28 days; however, for the mixtures containing pumice and zeolite, an increasing trend is observed in comparison to the plain mixture. Figure 3 indicates that the mixture containing 40% zeolite has superior performance among all the mixtures and, in comparison to the plain mixture, has 90% higher strength at the age of 90 days. The results show that substituting the limestone powder decreases the compressive strength at all ages, indicating that limestone powder could not be an effective SCMs for suppressing the conversion process in CAC system (Figure 4). The reason for this is that limestone acted only as a filler and ettringite and  $AH_3$  will form by reacting all CA with sulfate ions. This would result in decreased compressive strength [45].

Owing to the conversion process, porosity increases, and consequently, the strength decreases. In fact, during this process, the low-density metastable phases are changed to the stable phases with higher density [15]. It should be mentioned that the strength loss for the plain mixture is significantly higher than the mixture Z5, Z15, and P5, which shows that incorporating pumice and zeolite can mitigate

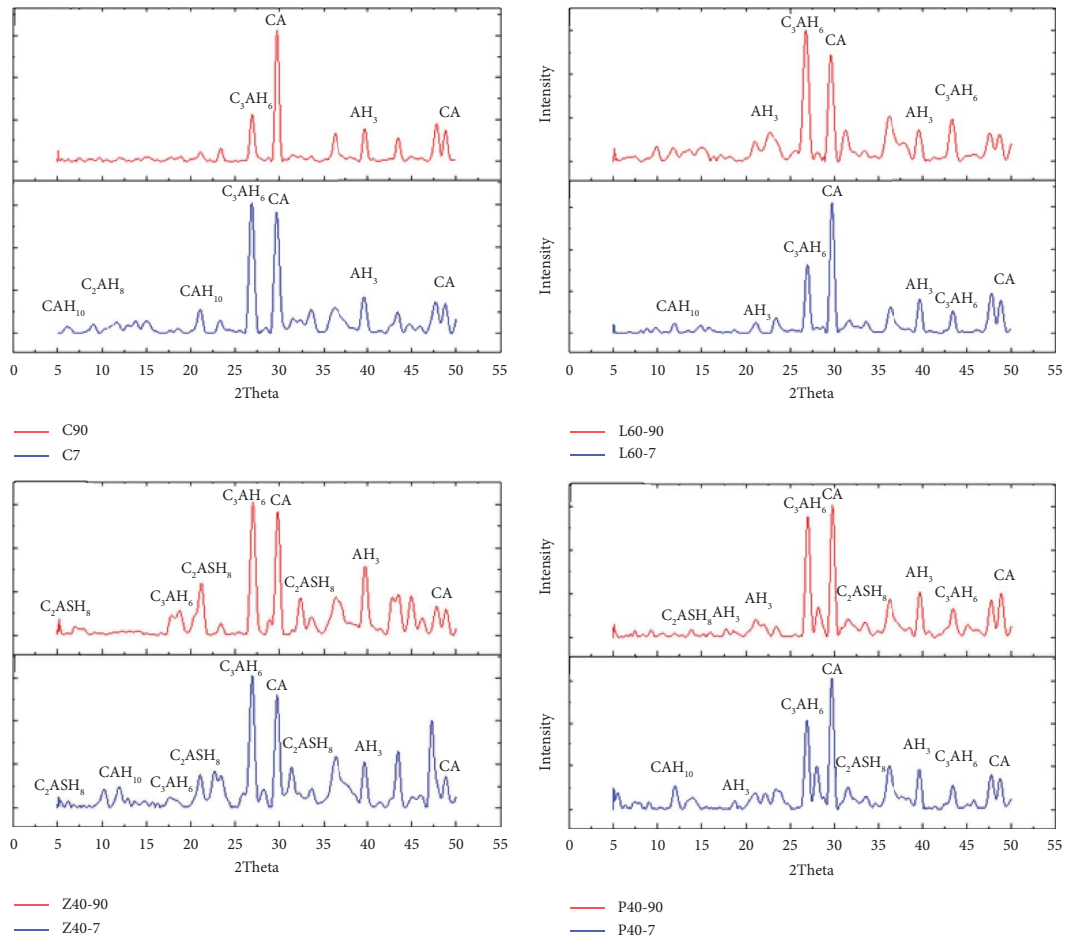


FIGURE 1: The X-ray diffraction patterns for the plain mixture and the mixtures containing 40% SCMs after 7 and 90 days of hydration.

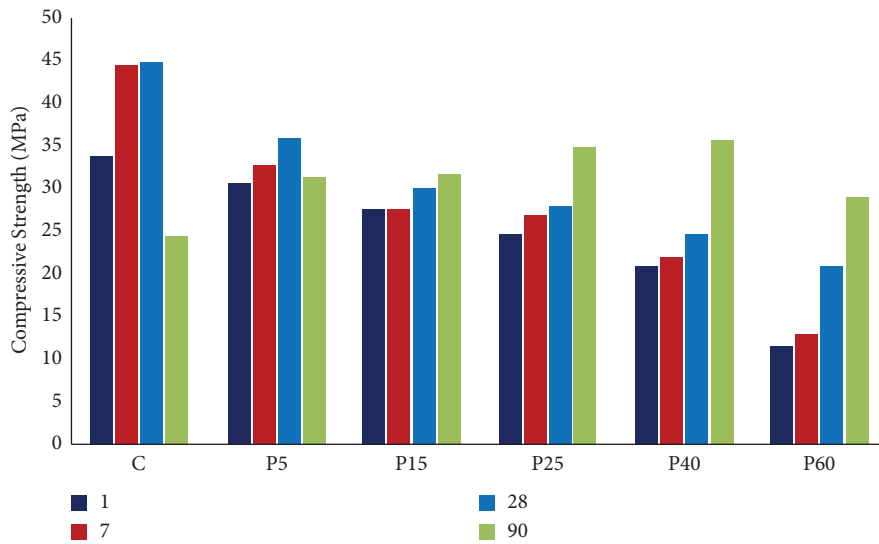


FIGURE 2: Compressive strength of the pumice mixtures at the age of 1 to 90 days.

the strength loss owing to the reaction of the silica content of pumice and zeolite with calcium aluminate hydrates. A hexagonal hydrate of alumina and silica known as gehlenite

or strätlingite has been proposed to form as a result of this reaction [13]. This reaction could avoid the conversion of hexagonal  $C_2AH_6$  to cubic  $C_3AH_6$ .

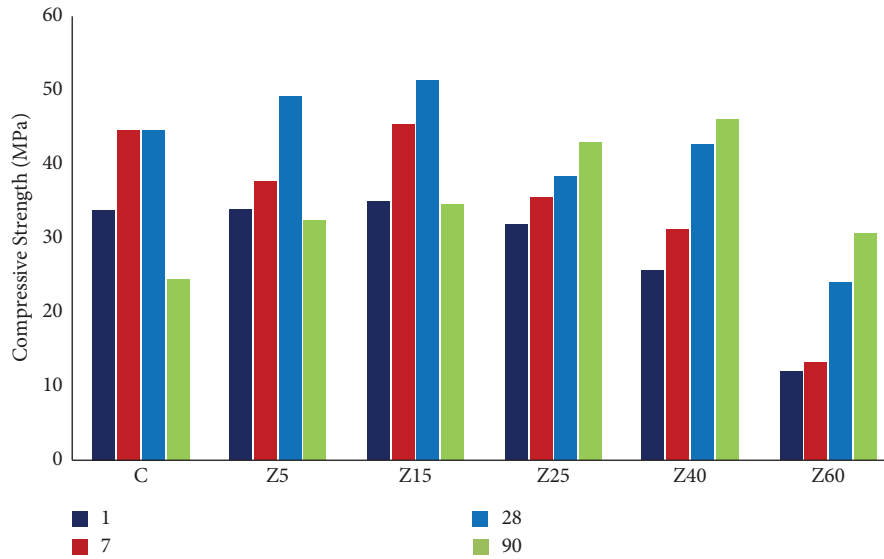


FIGURE 3: Compressive strength of the zeolite mixtures at the age of 1 to 90 days.

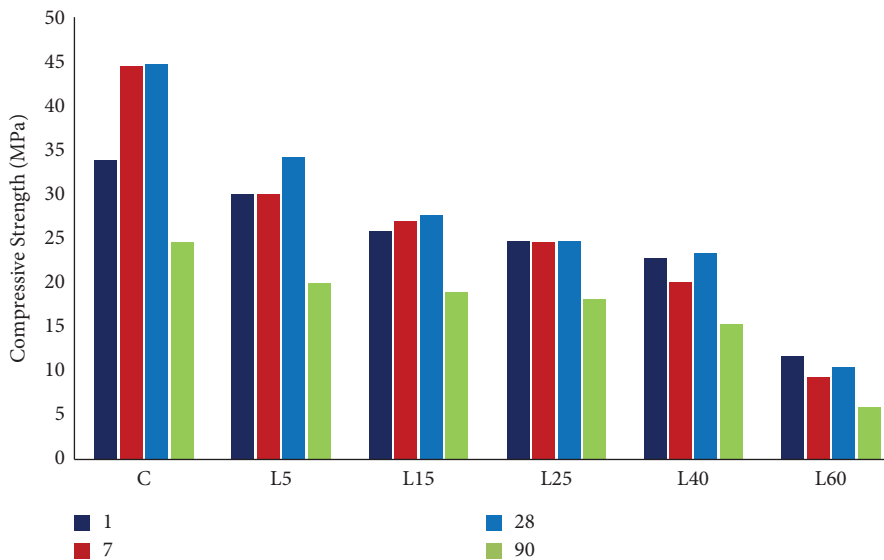


FIGURE 4: Compressive strength of the limestone mixtures at the age of 1 to 90 days.

Figure 2 shows that at the age of 90 days, the compressive strength is improved as the amount of pumice incorporation in CAC is increased up to 40%. At the age of 90 days, the compressive strength improvement for the P25, P40, and P60 is 25%, 45%, and 40%, respectively, compared to the age of 28 days. Moreover, similar trend is observed for the zeolite mixtures.

**3.3. Modulus of Rupture.** In Figures 5 and 6, the modulus of rupture of mixtures is presented at the ages of 28 and 90 days. At the age of 28 days, the plain mixture has the maximum modulus of rupture among the mixtures. Additionally, it should be mentioned that the mixtures containing 5% and 15% pumice and zeolite have similar

modulus of rupture to the plain mixture. However, by increasing the substitution level of pumice up to 60%, the modulus of rupture decreases significantly, which clearly shows that pumice powder does not have a significant reaction at this stage.

By increasing the age of mixtures from 28 days to 90 days, a different trend is observed. The plain mixture shows a significant reduction (16%) in modulus of rupture, which obviously shows that the conversion process has occurred at this age. Nevertheless, the mixtures containing pumice show an increasing trend in modulus of rupture. For instance, incorporation of 5%, 15%, 25%, 40%, and 60% pumice increases the modulus of rupture by about 23%, 44%, 95%, 152%, and 78% in comparison to the age of 28 days, respectively. This improvement may be because of the

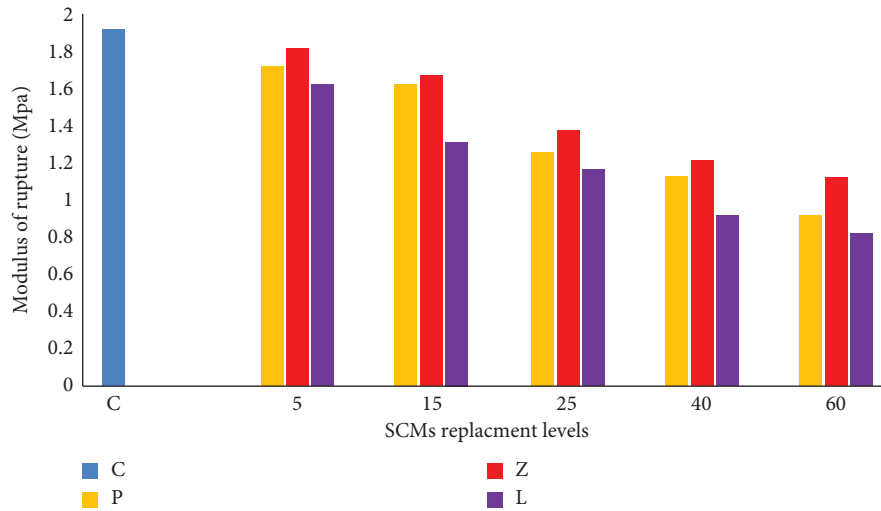


FIGURE 5: Modulus of rupture of the mixtures at the age of 28 days.

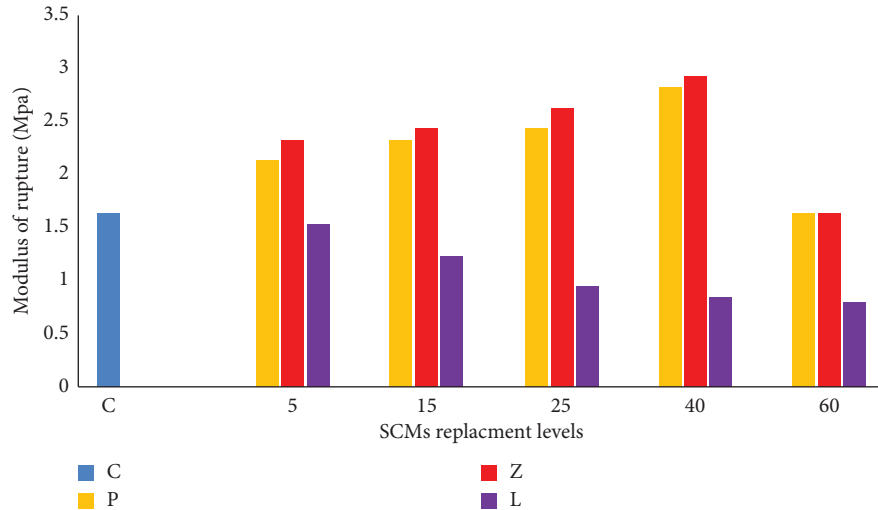


FIGURE 6: Modulus of rupture of the mixtures at the age of 90 days.

formation of the stable strätlingite phases and the mitigating effect of pumice on the conversion processes [46].

As it is clear from Figure 5, adding zeolite increases the modulus of rupture at the age of 90 days compared to the plain mixture. For instance, incorporation of 5%, 15%, 25%, 40%, and 60% zeolite leads to 28%, 45%, 91%, 142%, and 46% increases in modulus of rupture compared to the age of 28 days, respectively. It is also observed that the Z40 mixture has the optimum performance in comparison to all mixtures. Increasing the replacement level of zeolite at the age of 28 days decreases the modulus of rupture showing that zeolite does not have high reactivity at this age. It is noteworthy to mention that, at the age of 90 days, the mixtures containing 40% zeolite and pumice outperform the plain mixture by around 82% and 75% in modulus of rupture, respectively.

Figure 5 indicates the trend of modulus of rupture for different replacement levels of limestone powder. The results demonstrate that adding limestone leads to the reduction of

modulus of rupture, showing that limestone powder not only does not improve the modulus of rupture but also decreased it.

**3.4. Modulus of Elasticity.** Figure 7 shows the elastic modulus of mixtures at the age of 90 days. As it is clear, the incorporation of pumice and zeolite increases the elastic modulus of the mixtures compared to the plain mixture. For instance, the elastic modulus of mixtures containing 5%, 15%, 25%, 40%, and 60% pumice has increased by about 16%, 33%, 50%, 79%, and 8%, respectively, and for the mixtures containing 5%, 15%, 25%, 40%, and 60% zeolite has increased by about 50%, 54%, 71%, 96%, and 10% in comparison to the plain mixture, respectively. The mixture containing 40% zeolite has the best performance among all mixtures, which is compatible with the compressive and flexural strength results. Figure 7 shows that incorporating limestone powder decreases the modulus of elasticity.



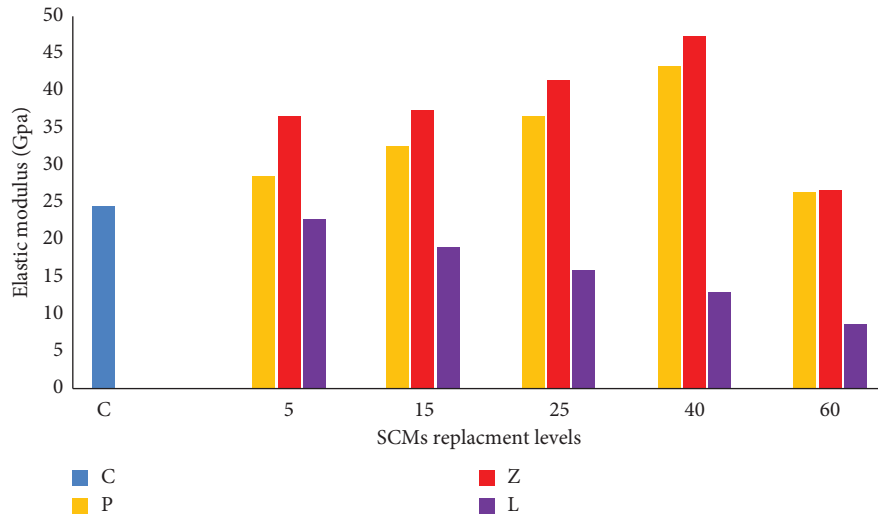


FIGURE 7: Modulus of elasticity of mixtures at the age of 90 days.

**3.5. Permeable Voids.** It is well known that the durability and mechanical properties of cement-based materials are highly influenced by the porosity. It should also be mentioned that the porosity in the cement matrix is dependent on the type of hydration products [14].

Figure 8 represents the permeable pore volume test results. As it can be observed at the age of 28 days, incorporating the high content of pumice, zeolite, and limestone powder has increased the permeable pore volume compared to the plain mixture. For instance, the incorporation of 5%, 15%, 25%, 40%, and 60% pumice increases the permeable pore volume by about 11%, 17%, 16%, 5%, and 25%, respectively. Furthermore, the incorporation of 5%, 15%, 25%, 40%, and 60% zeolite increases the permeable pore volume by about 9%, 14%, 15%, 3%, and 20%, respectively.

At the age of 28 days, the plain mixture has the lowest permeable pore space among all the mixtures, indicating a dense microstructure with lower porosity due to the formation of the metastable phases ( $\text{CAH}_{10}$  and  $\text{C}_2\text{AH}_8$ ). However, by increasing the age of mixtures from 28 days to 90 days, the plain mixture has an increasing trend (about 28%) in the volume of permeable pores showing that the conversion process has occurred. In the conversion process, the meta-stable phases with lower density are converted to the stable phases with higher density, which reduces the volume of solid, causing an increase in the porosity [14].

Despite the increased porosity in the plain mixture, the mixtures containing pumice and zeolite have a decreasing trend in the permeable pore volume. For example, the incorporation of 5%, 15%, 25%, 40%, and 60% pumice reduces by about 17%, 26%, 28%, 31%, and 25% of permeable pore volume compared to the plain mixture at the age of 90 days. In addition, the substitution of 5%, 15%, 25%, 40%, and 60% zeolite reduced approximately 21%, 31%, 33%, 35%, and 27% of permeable pore space compared to the plain mixture at the age of 90 days. Thus, pumice and zeolite significantly influence suppressing and mitigating of the conversion process. Nevertheless, at the age of 90 days, the addition of

limestone powder not only fails to reduce the volume of permeable pores but also increases it, which can be one of the reasons for the decrease in the mechanical properties of these mixtures compared to the plain mixture at the age of 28 days.

**3.6. Rapid Chloride Migration Test (RCMT).** Regarding durability, a critical problem in the chloride environment is the corrosion of rebar in concrete. Therefore, it is highly beneficial to examine the permeability of concrete in chloride environments. It should be mentioned that the chloride permeability coefficients of CAC cement composites have not been seriously investigated in the previous studies.

Replacing Portland cement with SCMs may significantly reduce the concrete diffusivity against aggressive ions [35]. However, this effect should also be comprehensively investigated in the CAC mixtures. As a matter of fact, SCMs affect the cement matrix via two main processes; they can act as a filler that seals the cement matrix as well as modify the characteristics and microstructure of the hydration product. The research [14] reveals that silica-containing minerals such as fly ash, blast furnace slag, and silica fume are capable of improving the CAC composites.

The results of RCMT test are depicted in Figure 9. At the age of 28 days, the mixtures incorporating pumice, zeolite, and limestone powder have a higher rapid chloride migration coefficient in comparison to the plain mixture. This phenomenon can be due to the nonoccurrence of the conversion process and also the low reactivity of pumice and zeolite at this age.

As it can be observed in Figure 10, at the age of 90 days, the maximum RCMT coefficients are observed for the L60 mixture with a value of  $12 \times 10^{-12} \text{m}^2/\text{s}$ , and the mixture with 40% zeolite has the lowest RCMT coefficient, which is  $0.9 \times 10^{-12} \text{m}^2/\text{s}$ . By increasing the age from 28 to 90 days, it is clear that the RCMT coefficient has been increased by 74% for the plain mixture, which shows the conversion process has occurred.

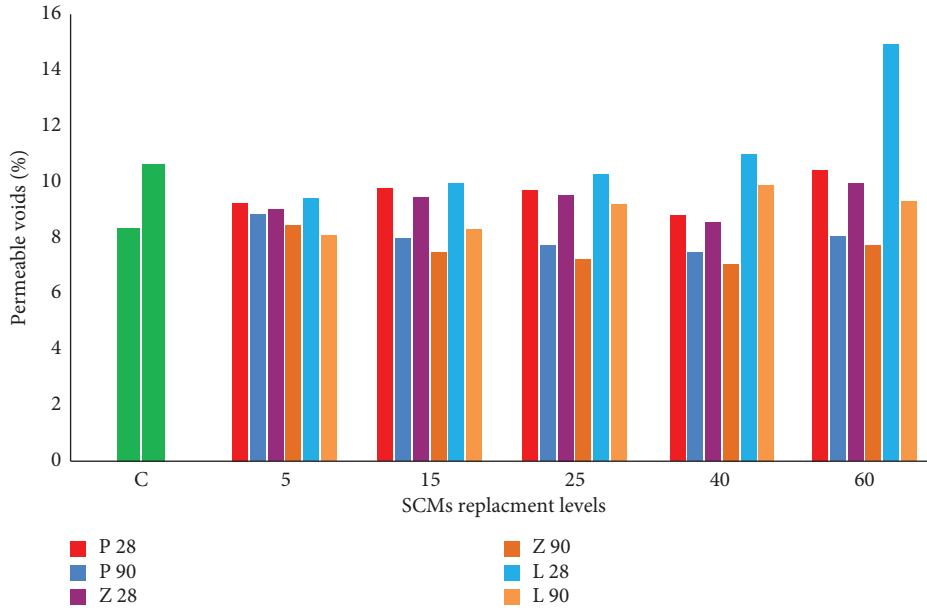


FIGURE 8: Permeable voids of the different mixtures at the age of 28 and 90 days.

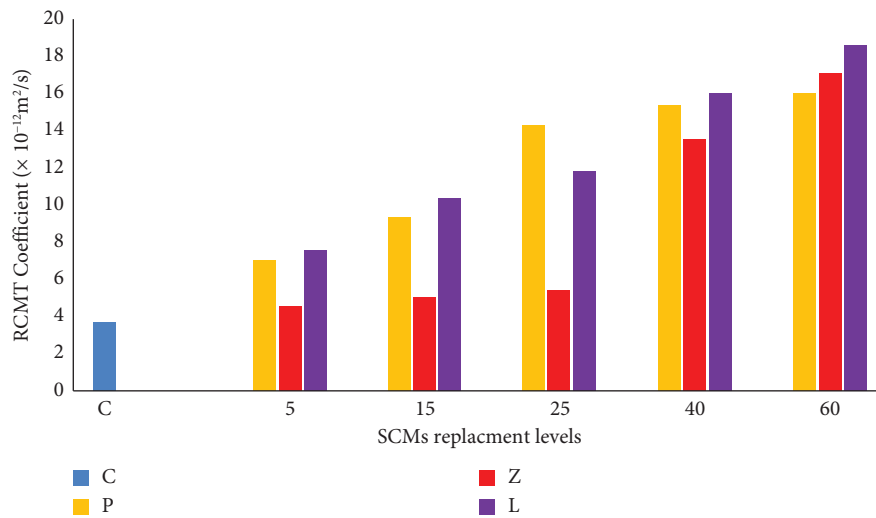


FIGURE 9: Rapid chloride migration test coefficient of the mixtures at the age of 28 days.

Using pumice mitigates the effect of the conversion process on the RCMT coefficient. For example, at the age of 90 days, the rapid chloride migration coefficients for the mixtures containing 5%, 15%, 25%, 40%, and 60% pumice are 28%, 49%, 69%, 91%, and 86% lower compared to the age of 28 days, respectively. As well, the zeolite has a positive effect on mitigating the conversion process and reducing the RCMT coefficient of mixtures. For instance, the rapid chloride migration coefficient for the mixtures containing 5%, 15%, 25%, 40%, and 60% zeolite shows 4%, 19%, 50%, 93%, and 92% reduction compared to the age of 28 days, respectively. It should be mentioned that mixtures containing 40% of zeolite and pumice had 85% and 78% lower

rapid chloride migration coefficients in comparison to the plain mixture at the age of 90 days.

In contrast to the mixtures containing pumice and zeolite, the RCMT coefficients of the composites containing limestone powder are increased, showing the low reactivity of the limestone powder in CAC based materials.

Mostafa et al. [47] showed that adding SCMs can inhibit the conversion reaction. Similarly, Heikal et al. [48] reported that adding slag to the CAC composite could inhibit the conversion process by forming strätlingite or gehlenite. As illustrated by equations (10) and (11), this is because the silica content of SCMs reacts with the main hydrate phases ( $\text{CAH}_{10}$  and  $\text{C}_2\text{AH}_8$ ) and forms the stable phase of strätlingite.

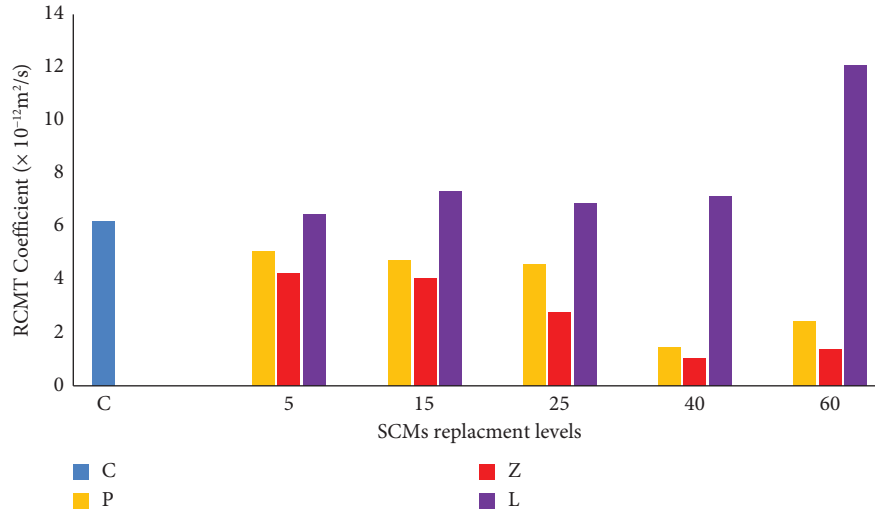
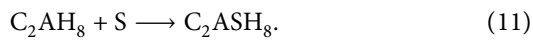
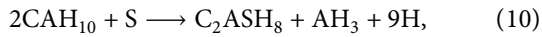


FIGURE 10: Rapid chloride migration test coefficient of the mixtures at the age of 90 days.



As shown in Figure 10, at the age of 90 days, incorporating pumice and zeolite reduced the RCMT coefficients owing to creating strätlingite phases instead of the metastable phases ( $\text{CAH}_{10}$  and  $\text{C}_2\text{AH}_8$ ) and acting as filler, which could fill the gaps in the cement matrix.

**3.7. Electrical Resistivity.** Electrical resistivity, which is a measure of the resistance of materials to the electrical current passage, has been considered as an index for investigating the durability of cement composites [49]. Measuring electrical resistivity provides valuable information for evaluating the corrosion risk of reinforcement.

As it is clear from Figures 11 to 13, at the age of 1 day, the plain mixture has the highest electrical resistivity among the mixtures. However, at this age, the mixtures incorporating 5%, 15%, 25%, and 40% pumice and zeolite have almost a similar electrical resistivity to that of the plain mixture. This high electrical resistivity is due to the formation of the metastable phases, which should be considered transient due to the conversion process occurrence by time. By increasing the age of the samples to 28 days, the plain and P5 mixture's electrical resistivity values are increased due to the hydration of the cement. However, in the mixtures containing 15%, 25%, 40%, and 60% pumice, the electrical resistivity is decreased, which might be as a result of lower cement for hydration and low reactivity of pumice powder to create strätlingite phases. In the mixtures containing zeolite, a different trend is observed in comparison to the pumice mixtures. The results show that by increasing the age of the specimens up to 28 days, the mixtures containing 5%, 15%, and 25% zeolite have similar electrical resistivity to the plain mixtures, and Z40 by reaching 98 k $\Omega$ -cm electrical resistivity has a significant increase in comparison to the plain mixture indicating the high reactivity of zeolite compared to pumice

and limestone powder. The electrical resistivity of mixtures containing limestone powder reveals that limestone powder did not improve the electrical resistivity due to low reactivity.

The research [50] indicates that curing time has a major impact on the surface electrical resistivity by virtue of the progressive hydration of Portland cement. As it can be seen in Figure 11, by increasing the age from 28 to 90 days, the electrical resistivity of the plain, P5, and P15 mixtures is reduced by about 60%, 55%, and 30%, respectively, which shows the significance of the conversion process. The occurrence of the conversion process increases the porosity of mixtures, which in turn can ease the flow of electrical current and reduce the electrical resistivity.

At the age of 90 days, the L5 mixture has the lowest electrical resistivity (16.4 k $\Omega$ -cm), and the mixture with 40% zeolite (Z40) has the highest electrical resistivity (167.2 k $\Omega$ -cm) among all the mixtures, which shows that zeolite has a significant effect on suppressing the conversion process. For instance, at the age of 90 days, the electrical resistivity values in the mixtures containing 25%, 40%, and 60% zeolite are improved by about 159%, 70%, and 73%, respectively, compared to the age of 28 days. Therefore, incorporating zeolite in a high replacement level improves the electrical resistivity and inhibits the occurrence of the conversion process. It is noteworthy to mention that the mixture containing 40% zeolite has about seven times the electrical resistance compared to the plain mixture at the age of 90 days.

It should be mentioned that using pumice also leads to improving the electrical resistivity. For example, in mixtures containing 25%, 40%, and 60% pumice, the electrical resistivity is enhanced by about 174%, 245%, and 200%, respectively. Figure 13 shows that adding limestone results in decreasing the electrical resistivity, which clearly indicates that limestone does not have a high reaction in CAC composite.

The electrical resistivity can be categorized into four groups. The electrical resistivity less than 10 k $\Omega$ -cm is considered as a high-risk corrosion, the electrical resistivity

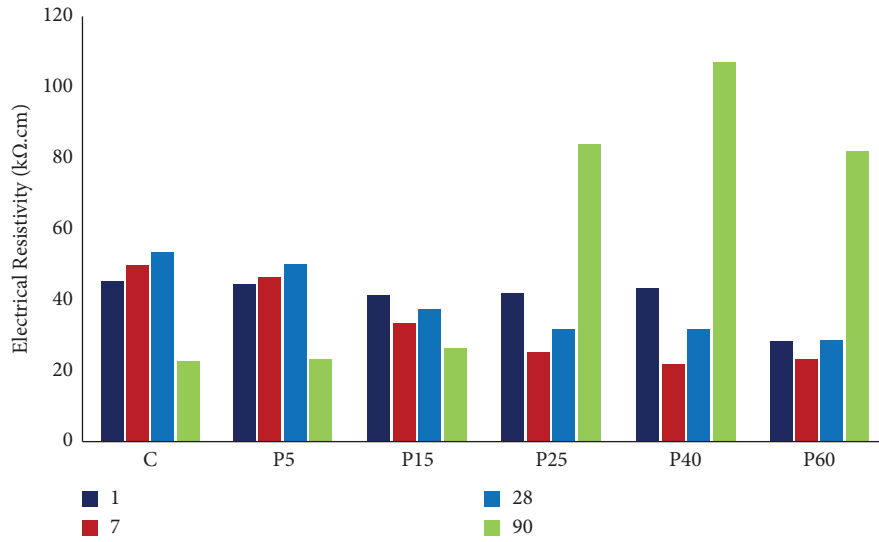


FIGURE 11: Electrical resistivity values of the pumice mixtures.

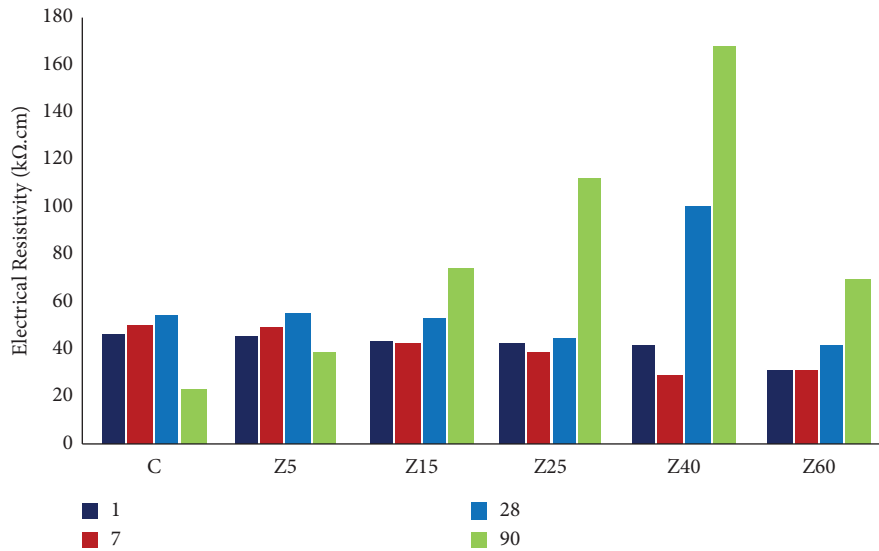


FIGURE 12: Electrical resistivity values of the zeolite mixtures.

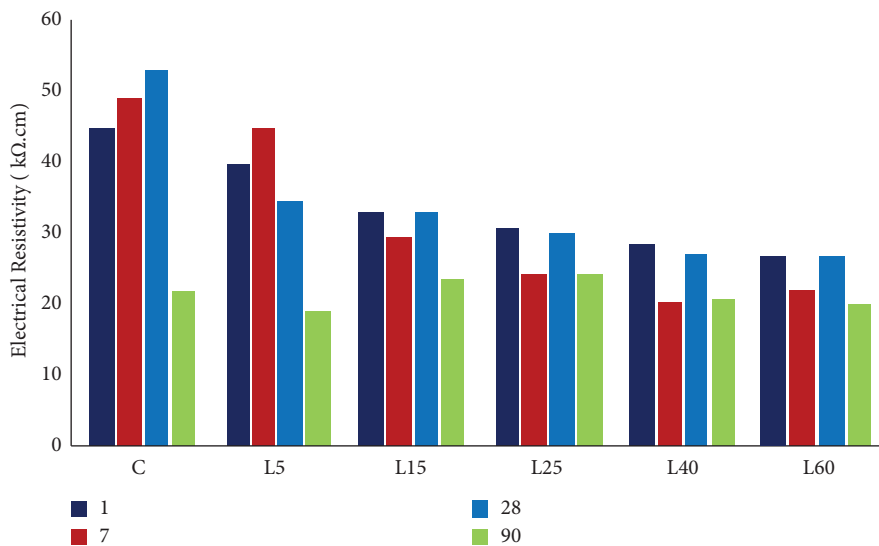


FIGURE 13: Electrical resistivity values of the limestone mixtures.

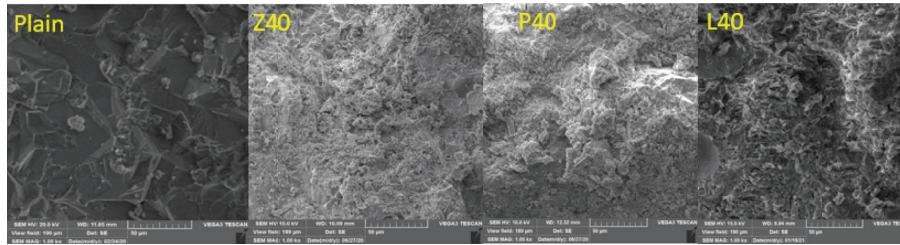


FIGURE 14: SEM images of plain, Z40, L40, and P40 mixture at the age of 28 days.

between 10–50 k $\Omega$ ·cm is considered as a moderate risk corrosion, and the electrical resistivity between 50–100 k $\Omega$ ·cm is considered as low-risk corrosion. For the electrical resistivity, more than 100 k $\Omega$ ·cm, the corrosion risk can be neglected [38]. As it is clear from Figures 11 to 13, the plain mixture and the mixtures containing 5% and 15% pumice and zeolite and all mixtures containing limestone powder can be categorized as the moderate risk of corrosion and the mixtures containing 25%, 60%, and 40% pumice and zeolite as the low and negligible risk of corrosion, respectively. Thus, using pumice and zeolite could notably improve the electrical resistivity of CAC composite and, accordingly, this durability index of CAC composite. It is worth mentioning that the result of electrical resistivity is compatible with other durability test results.

**3.8. SEM Analysis.** Figures 14 and 15 represent the scanning electron micrograph (SEM) of the mixtures. Figure 14 shows the microstructure of the mixtures at 28 days, which clearly indicates the densified cement matrix. This densified microstructure obviously shows that the conversion process has not been occurred significantly, which could be the reason for the high compressive strength of mixtures at this stage. Figure 15 indicates the SEM picture of the plain mixture at the age of 90 days. As it can be seen in Figure 15, due to the occurrence of the conversion process at this age, the micropores and microcracks are created in the plain and L40 mixtures, which could be a reason for the low mechanical and durability properties of these mixtures.

Generally, the strength is reduced as the porosity is increased in solids. The reason is that the solid part of the material resists external loads [14]. Additionally, it is known that porosity affects durability properties. The higher the porosity, the weaker the investigated durability properties [14]. Therefore, the increased porosity due to the conversion process can also explain the high permeability and low compressive strength of the plain and L40 mixtures at 90 days.

Figure 15 shows the SEM image of the mixture containing 40% pumice and zeolite. As it is demonstrated, the incorporation of 40% pumice and zeolite has improved the microstructure of the CAC composite. P40 and Z40 mixtures have a homogeneous and dense microstructure in comparison to the plain mixture. This can also support the higher compressive strength and improved durability properties of these mixtures.

In Figure 15, the stable phases are shown, and as it is clear, the  $C_3AH_6$  has a cubic structure while  $AH_3$  has a poorly crystalline structure, and the strätlingite phases have a platy structure [11, 51]. These two phases are responsible for the long-term properties of the CAC composite. As stated earlier, SCMs with a high silica content can react with metastable phases and create the strätlingite phases (stable phase), which is shown in Figure 15. This reaction can inhibit and mitigate the conversion process. The microstructural analysis is in agreement with the obtained durability results.

**3.9. Economic and Environmental Assessment.** This section evaluates the investigated mixture's unit cost and carbon footprint. The unit cost and carbon footprint of the mixes are computed using the aforementioned inventory data, as shown in Figures 16 and 17, and the plain mixture has the greatest overall cost as well as the largest quantity of GWP output in comparison to the other mixtures. As the SCMs replacement level increases, a downward trend is observed in the cost and quantity of GWP for all the mixtures.

As far as the environment is concerned, the results indicate that mixtures containing pumice outperformed mixtures containing zeolite and limestone powder. Moreover, the results show that using pumice, zeolite, and limestone powder significantly decreases the GWP index of mixtures compared to the plain mixture. The results indicate that the plain mixture produced 400 kg·m<sup>-3</sup> of carbon dioxide, while the mixture containing 60% zeolite, pumice, and limestone powder produced about 186,167, and 171 kg·m<sup>-3</sup> of carbon dioxide. Additionally, the P40 and Z40 mixtures, which are the optimum mixtures in this study, lower GWP index by 38% and 36%, respectively.

A key parameter in CAC's preference for construction practices is the cost of production. As a result, the cost of CAC composite has a substantial impact on its usage potential. Furthermore, as the above results demonstrate, the addition of pumice, zeolite, and limestone powder can significantly lower the cost of CAC composites. For instance, the usage of 60% pumice, zeolite, and limestone powder has resulted in a 50% reduction in the overall cost in comparison to the plain mixture. As mentioned earlier, one of the critical drawbacks of CAC cement is its high cost. The findings indicated that by utilizing SCMs, this issue might be significantly alleviated.

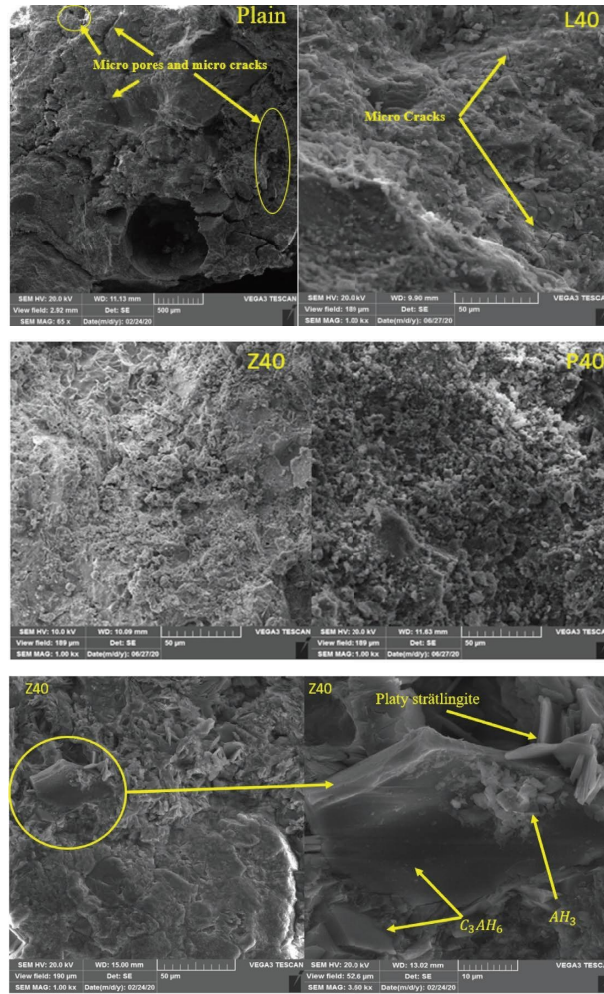


FIGURE 15: SEM images of plain, Z40, L40, and P40 mixture at the age of 90 days.

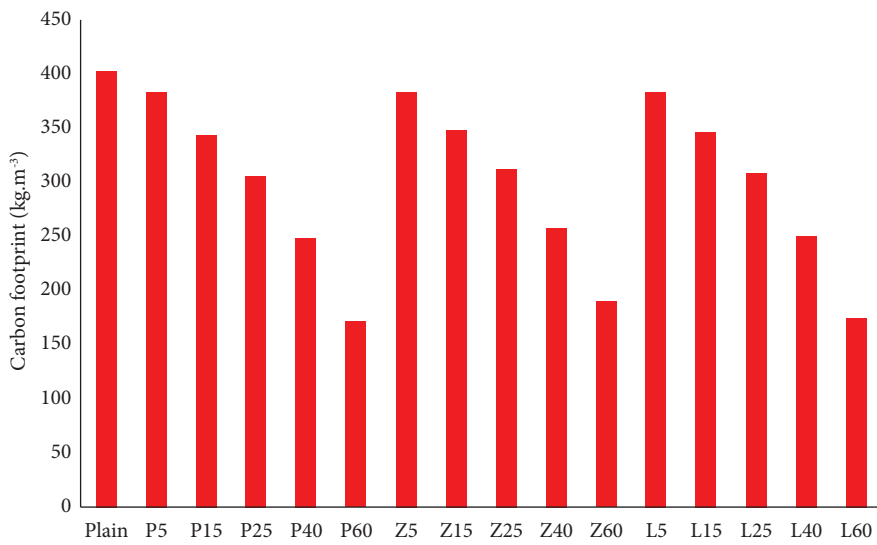


FIGURE 16: The global warming index (GWI) of mixtures per cubic meter concrete.



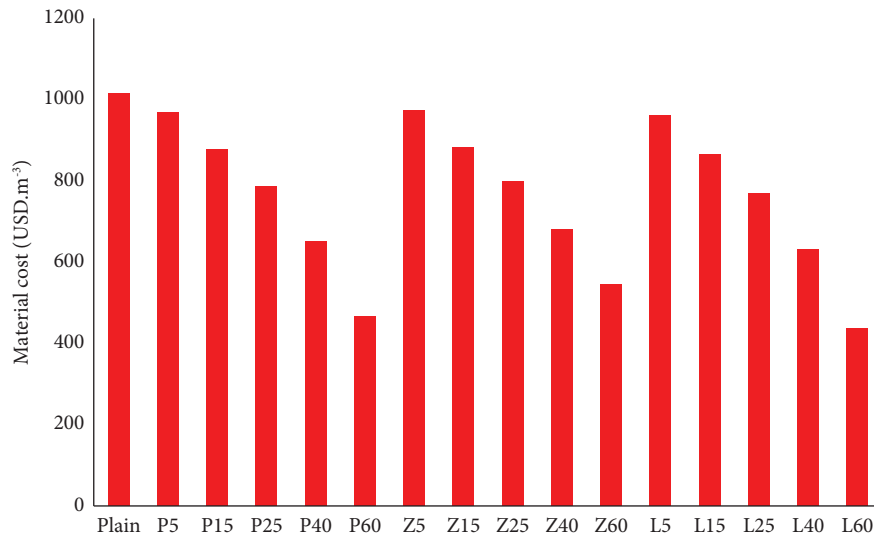


FIGURE 17: The total cost of mixtures per cubic meter concrete.

#### 4. Conclusion

This study investigates the effect of pumice, zeolite, and limestone powder on the mechanical, microstructural, and durability properties of CAC composites. For this purpose, 16 mixtures with different substitution levels of SCMs were prepared and evaluated. The most significant achievements of the present research can be summarized as follows:

- (i) The plain mixture reaches the compressive strength of 44 MPa at the age of 28 days; however, by increasing the age to 90 days, the compressive strength of the plain mixture was reduced to 24 MPa due to the occurrence of the conversion phenomenon. In addition, the modulus of rupture and electrical resistivity of the plain mixture decreased, respectively, by 16% and 60%. Meanwhile, the permeable pore space and the RCMT coefficient were increased by 28% and 74%.
- (ii) The results showed that in contrast to the plain mixture, the durability and mechanical properties of the CAC mixtures containing zeolite and pumice were enhanced. For instance, at the age 90 days, compressive strength, modulus of rupture, permeable pore space, electrical resistance, and RCMT coefficient for the P40 mixture were improved by 46%, 152%, 15%, 246%, and 92%, respectively, in comparison to the age 28 days, and for the Z40 mixture were enhanced by 9%, 141%, 18%, 70%, and 94%, respectively. This improvement maybe because of the formation of the stable strätlingite phases and the mitigating effect of pumice and zeolite on the conversion processes. Moreover, it is noteworthy to mention that even mixes containing 60% zeolite and pumice can be used in structural concrete.
- (iii) Microstructural analysis reveals that the P40 and Z40 mixtures have a homogeneous and densified microstructure in comparison to the plain mixture,

showing that pumice and zeolite incorporation could limit the conversion process and can improve the microstructure of CAC composite. XRD analysis demonstrated that pumice and zeolite were capable of reducing conversion processes and that limestone powder did not work well in the CAC composites.

- (iv) Based on the results of economic and environmental analyses, SCMs significantly reduce the final cost of CAC production as well as greenhouse gas emissions. Moreover, the P40 and Z40 mixtures, which were the optimum mixtures in this study, lowered GWP index by 38% and 36%, respectively.

#### Data Availability

The data supporting the current study are available from the corresponding author upon request.

#### Conflicts of Interest

The authors declare that they have no conflicts of interest.

#### References

- [1] M. V. J. P. Bayoux, J. P. Letourneux, and S. Marcdargent, "International Symposium Calcium aluminate cement conversion analysed," in *Acidic Corrosion of High Alumina Cement*, R. J. Mangabhai, Ed., E. F. N. Spon, London, UK, 2014.
- [2] J. P. L. C. Parr, D. Verat, and C. Wohrmeyer, "High purity calcium aluminate binders for demanding high temperature applications," in *Proceedings of the Centenary Conference Calcium Aluminate Cement*, Avignon, France, June 2008.
- [3] H. G. Midgley, *High Alumina Cement in Construction - a Future Based on Experience, International Symposium on Calcium Aluminate Cements*, E & F. N. Spon, London, UK, 1990.
- [4] A. Goyns, "Calcium aluminate cement linings for cost-effective sewers," In *CAC: Calcium Aluminate Cements 200*, pp. 617–631, Edinburgh, 2001.

- [5] A. Goyns, "Calcium aluminate cement linings for cost-effective sewers," *Calcium Aluminate Cem*, pp. 617–631, 2001.
- [6] K. L. Scrivener, J. L. Cabiron, and R. Letourneux, "High-performance concretes from calcium aluminate cements," *Cement and Concrete Research*, vol. 29, no. 8, pp. 1215–1223, 1999.
- [7] M. Goyns and M. Alexander, "Performance of various concretes in the Virginia experimental sewer over 20 years," in *Proceedings of the International conference on calcium aluminate cements*, pp. 573–584, Avignon, France, May 2014.
- [8] F. G. C. M. Williams, *Recycling/Reclaiming a Savings Spree: Chicago Reuses to the max on Famous Shopping Mile, Illinois Interchang*, Illinois Department of Transportation, Springfield, IL, USA, 2009.
- [9] TxDoT Ss-4491 Class Cac Concrete, *Texas Department of Transportation*, Texas Department of Transportation Austin, Austin, TX, 2009.
- [10] M. C. G. Juenger, F. Winnefeld, J. L. Provis, and J. H. Ideker, "Advances in alternative cementitious binders," *Cement and Concrete Research*, vol. 41, no. 12, pp. 1232–1243, 2011.
- [11] H. Pollmann, "Calcium aluminate cements - raw materials, differences, hydration and properties," *Reviews in Mineralogy and Geochemistry*, vol. 74, pp. 1–82, 2012.
- [12] A. Scrivener and Capmas, "Lea's chemistry of cement and concrete," *Calcium aluminate cements*, vol. 69, 1998.
- [13] C. Gosselin, *Microstructural Development of Calcium Aluminate Cement Based Systems with and without Supplementary Cementitious Materials (No. THESIS)*, EPFL, Lausanne, Switzerland, 2009.
- [14] A. C. Scrivener, "Calcium aluminate cements," in *Lea's Chemistry of Cement and concrete*, P. C. Hewlet, Ed., 2004.
- [15] M. P. Adams and J. H. Ideker, "Influence of aggregate type on conversion and strength in calcium aluminate cement concrete," *Cement and Concrete Research*, vol. 100, pp. 284–296, 2017.
- [16] S. Bushnell-Watson and U. Research, *The Effect of Temperature upon the Setting Behaviour of Refractory Calcium Aluminate Cements*, Elsevier, Amsterdam, Netherlands, 1986.
- [17] S. M. Bushnell-Watson and J. H. Sharp, "Further studies of the effect of temperature upon the setting behaviour of refractory calcium aluminate cements," *Cement and Concrete Research*, vol. 20, no. 4, pp. 623–635, 1990.
- [18] S. M. Bushnell-Watson and J. H. Sharp, "La aplicación de análisis térmico a las reacciones de hidratación y conversión de cementos aluminosos," *Materiales de Construcción*, vol. 42, no. 228, pp. 13–32, 1992.
- [19] S. M. Bushnell-Watson and J. H. Sharp, "On the cause of the anomalous setting behaviour with respect to temperature of calcium aluminate cements," *Cement and Concrete Research*, vol. 20, no. 5, pp. 677–686, 1990.
- [20] V. Antonovič, J. Keriene, R. Boris, and M. Aleknevičius, "The effect of temperature on the formation of the hydrated calcium aluminate cement structure," *Procedia Engineering*, vol. 57, pp. 99–106, 2013.
- [21] D. K. Panesar and R. Zhang, "Performance comparison of cement replacing materials in concrete: limestone fillers and supplementary cementing materials – a review," *Construction and Building Materials*, vol. 251, Article ID 118866, 2020.
- [22] G. L. Golewski, "The influence of microcrack width on the mechanical parameters in concrete with the addition of fly ash: consideration of technological and ecological benefits," *Construction and Building Materials*, vol. 197, pp. 849–861, 2019.
- [23] G. L. Golewski, "An assessment of microcracks in the Interfacial Transition Zone of durable concrete composites with fly ash additives," *Composite Structures*, vol. 200, pp. 515–520, 2018.
- [24] H. P. Maarten and A. T. M. Broekmans, *Applied Mineralogy of Cement & Concrete*, 1 edition, Walter de Gruyter GmbH & Co KG, 2012.
- [25] A. F. Bentivegna, *Multi-scale Characterization, Implementation, and Monitoring of Calcium Aluminate Cement Based-systems(Doctoral Dissertation)*, The University of Texas at Austin, 2012.
- [26] O. Kirca, I. Ozgür Yaman, and M. Tokyay, "Compressive strength development of calcium aluminate cement–GGBFS blends," *Cement and Concrete Composites*, vol. 35, no. 1, pp. 163–170, 2013.
- [27] M. Collepardi, S. Monosi, and P. Piccioli, "The influence of pozzolanic materials on the mechanical stability of aluminous cement," *Cement and Concrete Research*, vol. 25, no. 5, pp. 961–968, 1995.
- [28] C. ASTM, *Standard Test Method for Flow of Hydraulic Cement Mortar, C1437*, 2007.
- [29] EN, B. S. *Testing Hardened Concrete-Part 3: Compressive Strength of Test Specimens*, British Standard Institution, London, UK, 2009.
- [30] N. T. Nordtest, *BUILD 492. Chloride Migration Coefficient from Non-steady-state Migration Experiments*, Nordtest, Alessandria, Finland, 1999.
- [31] J. W. Lencioni and M. G. de Lima, "A study of the parameters that affect the measurements of superficial electrical resistivity of concrete," *RILEM Bookseries*, vol. 6, pp. 271–276, 2013.
- [32] K. R. Gowers and S. G. Millard, "Measurement of concrete resistivity for assessment of corrosion severity of steel using wenner technique," *ACI Materials Journal*, vol. 96, pp. 536–541, 1999.
- [33] Standard, "Methods of testing cement," *Determination of Strength*, 2005.
- [34] Astm C 469, *ASTM C469/C469M-14: Standard Test Method for Static Modulus of Elasticity and Poisson's Ratio of concrete in Compression*, Annual Book of ASTM Standards, Pennsylvania, PA, USA, 2014.
- [35] ASTM International, *Standard Test Method for Density, Absorption, and Voids in Hardened concrete*, 2013.
- [36] X. Li, X. Lv, X. Zhou, W. Meng, and Y. Bao, "Upcycling of waste concrete in eco-friendly strain-hardening cementitious composites: mixture design, structural performance, and life-cycle assessment," *Journal of Cleaner Production*, vol. 330, Article ID 129911, 2022.
- [37] H. Madani, M. N. Norouzfifar, and J. Rostami, "The synergistic effect of pumice and silica fume on the durability and mechanical characteristics of eco-friendly concrete," *Construction and Building Materials*, vol. 174, pp. 356–368, 2018.
- [38] M. Valipour, M. Yekkalari, M. Shekarchi, and S. Panahi, "Environmental assessment of green concrete containing natural zeolite on the global warming index in marine environments," *Journal of Cleaner Production*, vol. 65, pp. 418–423, 2014.
- [39] E. Henry-Lanier, M. Szepizdyn, and C. Parr, "Optimisation of the environmental footprint of calcium-aluminate-cement containing castables," *Refractories Worldforum*, vol. 8, no. 3, pp. 81–86, 2015.
- [40] J. Rostami, O. Khandel, R. Sedighardekani, A. R. Sahneh, and S. Ghahari, "Enhanced workability, durability, and thermal properties of cement-based composites with aerogel and



- paraffin coated recycled aggregates,” *Journal of Cleaner Production*, vol. 297, Article ID 126518, 2021.
- [41] D. A. Salas, A. D. Ramirez, N. Ulloa, H. Baykara, and A. J. Boero, “Life cycle assessment of geopolymers concrete,” *Construction and Building Materials*, vol. 190, pp. 170–177, 2018.
- [42] H. M. Son, S. M. Park, J. G. Jang, and H. K. Lee, “Effect of nano-silica on hydration and conversion of calcium aluminate cement,” *Construction and Building Materials*, vol. 169, pp. 819–825, 2018.
- [43] Y. T. Tran, J. Lee, P. Kumar, K.-H. Kim, and S. S. Lee, “Natural zeolite and its application in concrete composite production,” *Composites Part B: Engineering*, vol. 165, pp. 354–364, 2019.
- [44] F. A. Sabet, N. A. Libre, and M. Shekarchi, “Mechanical and durability properties of self-consolidating high performance concrete incorporating natural zeolite, silica fume and fly ash,” *Construction and Building Materials*, vol. 44, pp. 175–184, 2013.
- [45] J. Bizzozero and K. L. Scrivener, “Limestone reaction in calcium aluminate cement–calcium sulfate systems,” *Cement and Concrete Research*, vol. 76, pp. 159–169, 2015.
- [46] K. Şengül and S. T. Erdoğan, “Influence of ground perlite on the hydration and strength development of calcium aluminate cement mortars,” *Construction and Building Materials*, vol. 266, no. 2021, Article ID 120943, 2021.
- [47] N. Y. Mostafa, Z. I. Zaki, and O. H. Abd Elkader, “Chemical activation of calcium aluminate cement composites cured at elevated temperature,” *Cement and Concrete Composites*, vol. 34, no. 10, pp. 1187–1193, 2012.
- [48] M. Heikal, M. S. Morsy, and M. M. Radwan, “Electrical conductivity and phase composition of calcium aluminate cement containing air-cooled and water-cooled slag at 20, 40 and 60 °c,” *Cement and Concrete Research*, vol. 35, no. 7, pp. 1438–1446, 2005.
- [49] R. Kurda, J. De Brito, and J. D. Silvestre, “Water absorption and electrical resistivity of concrete with recycled concrete aggregates and fly ash,” *Cement and Concrete Composites*, vol. 95, pp. 169–182, 2019.
- [50] G. J. L. Coppio, M. G. De Lima, J. W. Lencioni, L. S. Cividanes, P. P. O. L. Dyer, and S. A. Silva, “Surface electrical resistivity and compressive strength of concrete with the use of waste foundry sand as aggregate,” *Construction and Building Materials*, vol. 212, pp. 514–521, 2019.
- [51] J. F. Zapata, H. A. Colorado, and M. A. Gomez, “Effect of high temperature and additions of silica on the microstructure and properties of calcium aluminate cement pastes,” *Journal of Sustainable Cement-Based Materials*, vol. 9, pp. 323–349, 2020.